PLANT SCIENCES

Optogenetic control of the guard cell membrane potential and stomatal movement by the light-gated anion channel *Gt*ACR1

Shouguang Huang[1†], Meiqi Ding[1†], M. Rob G. Roelfsema[1]*, Ingo Dreyer[2], Sönke Scherzer[1], Khaled A. S. Al-Rasheid[3], Shiqiang Gao[1,4], Georg Nagel[1,4], Rainer Hedrich[1]*, Kai R. Konrad[1]*

Guard cells control the aperture of plant stomata, which are crucial for global fluxes of CO_2 and water. In turn, guard cell anion channels are seen as key players for stomatal closure, but is activation of these channels sufficient to limit plant water loss? To answer this open question, we used an optogenetic approach based on the light-gated anion channelrhodopsin 1 (*Gt*ACR1). In tobacco guard cells that express *Gt*ACR1, blue- and green-light pulses elicit Cl^- and NO_3^- currents of −1 to −2 nA. The anion currents depolarize the plasma membrane by 60 to 80 mV, which causes opening of voltage-gated K^+ channels and the extrusion of K^+. As a result, continuous stimulation with green light leads to loss of guard cell turgor and closure of stomata at conditions that provoke stomatal opening in wild type. *Gt*ACR1 optogenetics thus provides unequivocal evidence that opening of anion channels is sufficient to close stomata.

INTRODUCTION

Approximately half of the terrestrial rainfall is returned by plants to the atmosphere via small pores in the leaf surface (*1*). These stomatal pores act as valves that open to enable uptake of CO_2 for photosynthesis and close to protect plants from uncontrolled water loss (*2*, *3*). Consequently, stomata have an enormous impact on global fluxes of CO_2 and water. Understanding the mechanisms that regulate stomatal movements, therefore, is pivotal to improve climate models and develop strategies to reduce water consumption in agriculture (*4*, *5*).

Stomata are formed by pairs of guard cells that can sense the intercellular CO_2 concentration of leaves and the stress hormone ABA, which is a proxy for a low water status in plants. Both high CO_2 and ABA levels cause stomatal closure by inducing the efflux of ions from guard cells. Because of the loss of osmolites, the guard cells shrink and cause closure of the stomatal pore (*6*, *7*). This impact of CO_2 and ABA on stomata has been linked to their ability to control the activity of several ion transport proteins in guard cells, including K^+ channels, anion channels, and H^+-dependent adenosine triphosphatases (H^+-ATPases) (*2*, *8*, *9*). However, the relative contribution of each of these transporters to CO_2- and ABA-induced stomatal closure has remained unresolved.

The discovery of light-gated ion channels has revolutionized neurobiological research (*10*–*12*), and three such tools were recently introduced in plant science (*13*–*15*). Two rhodopsin-based channels were shown to facilitate light-induced depolarizations in plant cells (*14*, *15*), while the light-activated K^+ channel BLINK1 (blue light-induced K^+ channel 1) accelerated stomatal closure and opening. As a result, BLINK1 enhanced the water usage efficiency of plants that were exposed to rapidly changing environmental conditions (*13*). However, light activation of BLINK1 did not necessarily cause stomatal closure, which suggests that opening of K^+ channels is not the key that initiates this process.

On the basis of the phenotypes of loss-of-function mutants, the slow anion channel-associated 1 (SLAC1)–type channels seem to be major players in ABA- and CO_2-induced stomatal closure (*16*–*19*). However, it is not known whether activation of these channels is sufficient to provoke the efflux of anions and K^+ from guard cells, which is supposed to close stomatal pores. We therefore selected *Gt*ACR1, a light-gated anion channelrhodopsin of the algae *Guillardia theta* (*20*, *21*) that was recently shown to provoke large membrane depolarizations in plants (*15*). Here, we show that the light-dependent activation of *Gt*ACR1 in tobacco guard cells evoked anion currents of −1 to −2 nA, depolarized the plasma membrane, and also provoked a release of K^+. As a consequence of the combined anion and cation release, stomata closed and the transpiration of leaves declined. Our *Gt*ACR1-based optogenetic approach thus documents that the activation of plasma membrane anion channels is sufficient to trigger rapid stomatal closure. These results point to the endogenous anion channels in guard cells as prime targets for breeding of water saving plants.

RESULTS

Light pulses rapidly depolarize guard cells that express *Gt*ACR1

Guard cells use plasma membrane anion channels to provoke prolonged membrane depolarizations (*18*, *22*, *23*). The light-activated anion channel from the cryptophyte alga *Guillardia theta* (*Gt*ACR1) may mimic this function because *Gt*ACR1 strictly conducts anions, just like plant S-type anion channels (*20*, *23*). Recently, tobacco plants were transformed with an improved version of *Gt*ACR1 and the marine bacterial β-carotene 15, 15′-dioxygenase (MbDio) (*15*). The expression of both genes was controlled by a single UBQ10 promotor, and the proteins were posttranscriptionally separated by a P2A self-cleavage site. While *Gt*ACR1 was targeted to the plasma

[1]Molecular Plant Physiology and Biophysics, Julius-von-Sachs Institute for Biosciences, Biocenter, Würzburg University, Julius-von-Sachs-Platz 2, D-97082 Würzburg, Germany. [2]Center of Bioinformatics, Simulation and Modeling (CBSM), Faculty of Engineering, Universidad de Talca, 2 Norte 685, 3460000 Talca, Chile. [3]Zoology Department, College of Science, King Saud University, 11451 Riyadh, Saudi Arabia. [4]Institute of Physiology, Würzburg University, Röntgenring 9, 97070 Würzburg, Germany.
*Corresponding author. Email: hedrich@botanik.uni-wuerzburg.de (R.H.); roelfsema@botanik.uni-wuerzburg.de (M.R.G.R); kai.konrad@botanik.uni-wuerzburg.de (K.R.K)
†These authors contributed equally to this work.

membrane, MbDio entered the chloroplast and produced all-trans retinal from β-carotene, which is an essential cofactor for rhodopsins. The in planta biosynthesis of retinal facilitates the use of rhodopsin-based optogenetics in intact plants (*15*).

The transcript dosage of *Gt*ACR1, tagged with enhanced yellow fluorescent protein (eYFP), was studied for guard cells in two tobacco lines (Ret-ACR1 2.0 lines #1 and #2) and compared to control plants that only expressed eYFP and MbDio. The analysis of mechanically isolated guard cells (*24*) confirmed that the stomatal development transcription factor *Nt*FAMA1 was preferentially expressed in these motor cells (fig. S1A) (*25*). A high guard cell expression level was also found for the K^+ solanum transporter (K^+ channel) *Nt*KST1 (fig. S1B) (*26*, *27*), the *Nt*SLAC1 (fig. S1C) (*16*, *17*), and the guard cell outward rectifying K^+ channel *Nt*GORK (fig. S1D) (*28*). Transcripts of the *Gt*ACR1-eYFP were not detected in control plants but were detected in guard cells of lines #1 and #2, with an approximately twofold higher expression in line #1, as in line #2 (Fig. 1A). In agreement with these data, strong yellow fluorescent signals were recognized in the periphery of guard cells of lines #1 and #2 (Fig. 1B), while a control line with untagged eYFP showed a bright fluorescence signal in the cytosol and nucleus (Fig. 1B). The *Gt*ACR1 channel is thus localized to the plasma membrane of guard cells of both lines, just as previously found for epidermal leaf cells and pollen tubes (*15*).

Guard cells are naturally disconnected from their neighbors (*29*), and because of this unique property, the activity of their ion channels can be monitored in intact plants (*30*, *31*). Microelectrodes were impaled into guard cells to monitor light-induced changes in transmembrane potential and current.

Blue-light (BL) pulses were applied in addition to a continuous red-light background illumination (Fig. 1, C and D). Pulses with a duration of 0.1 s did not affect the control cells but triggered a rapid and strong depolarization of *Gt*ACR1-expressing guard cells, which was reversed after termination of BL illumination (Fig. 1C). Guard cells could be repetitively stimulated with BL pulses with a duration of 0.1, 1, or 10 s (Fig. 1D). These trains of BL pulses provoked a series of depolarizations with a constant magnitude of approximately 70 mV in line #1 (Fig. 1, D and E) and 50 mV in line #2 (Fig. 1E and fig. S2). Note that, during the longest BL pulses of 10 s, a partial repolarization of the free running membrane potential (E_m) occurred to approximately −80 mV. This poststimulation effect indicates that a guard cell endogenous current (studied below) counteracts the depolarization triggered by the activation of *Gt*ACR1 (Fig. 1D, right).

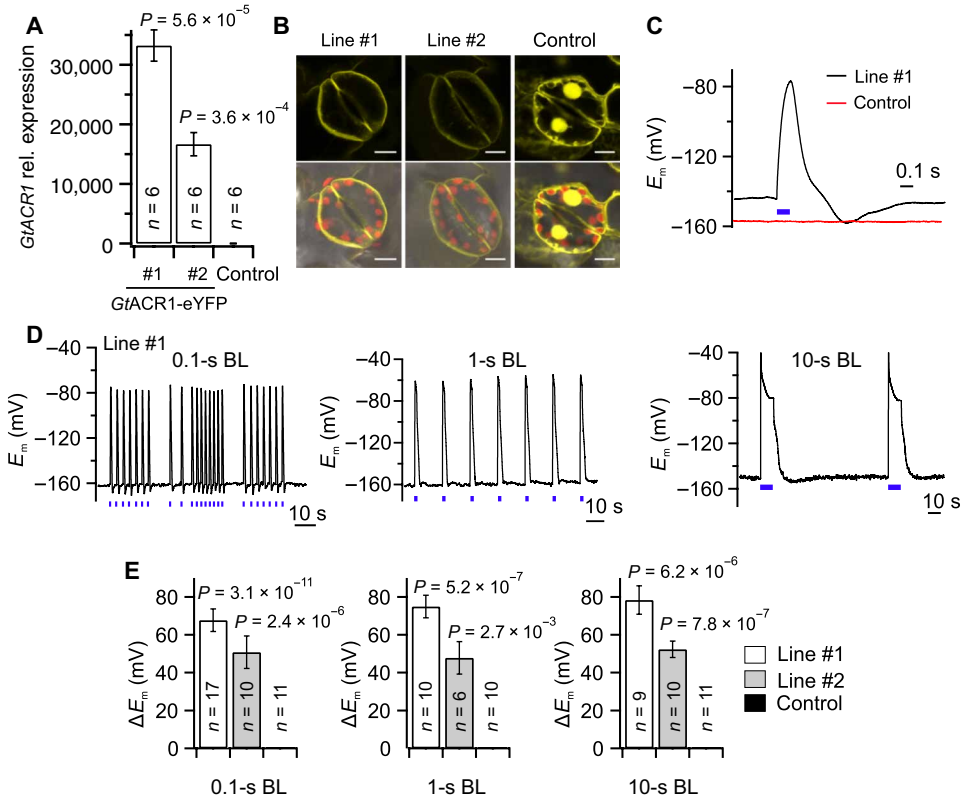

Fig. 1. *Gt*ACR1 depolarizes the plasma membrane of tobacco guard cells in response to BL pulses. (**A**) Transcript levels of *Gt*ACR1-eYFP in guard cells, of two tobacco *Gt*ACR1-transformed lines (#1 and #2) and a control line. The transcript numbers of *Gt*ACR1 were normalized to 10,000 molecules of actin. (**B**) Fluorescence signals of eYFP linked to *Gt*ACR1 in line #1 (left upper panel) and #2 (middle upper panel) or free eYFP (right upper panel) in control tobacco guard cells and the overlay with the chlorophyll fluorescence signal in the corresponding lower panels. Scale bars, 10 μm. (**C**) Membrane potential recordings of tobacco guard cells of line #1 (black curve) and control (red curve) stimulated with a single blue light (BL) pulse of 0.1 s (as shown by the blue bar, λ = 470 nm, 17 mW/mm^2). (**D**) Membrane potential measurements of tobacco guard cells (line #1) stimulated with BL pulses of 0.1, 1, and 10 s (λ = 470 nm, 17 mW/mm^2), as indicated by the blue bars below the traces. (**E**) Average depolarization of guard cells in line #1, line #2, and control provoked by BL pulses of 0.1, 1, and 10 s. In (A) and (E), the *P* values were determined with a Student's *t* test using values of *Gt*ACR1 line #1 or #2 and control plants; the number of experiments is given in the respective bars, and error bars represent SE.

Light-activated *Gt*ACR1 channels conduct monovalent anions

The ability of *Gt*ACR1 to depolarize guard cells suggests that it can be used as a light-controlled stand-in for the guard cell intrinsic anion channels. Given that the stress hormone ABA triggers plasma membrane anion currents of approximately −200 pA in guard cells of *Vicia faba* (*32*) and tobacco (*31*), it is likely that currents of this magnitude are required for rapid stomatal closure. We therefore tested whether the conductance of *Gt*ACR1 fulfills this requirement. Guard cells were impaled with double-barreled microelectrodes, of which one barrel monitored the membrane potential, whereas the second was used to inject ion currents and clamp the plasma membrane to −100 mV. In this configuration, repetitive BL pulses with durations of 0.1, 1, or 10 s provoked sequential current spikes with a peak amplitude of approximately −2 nA in line #1 and −1 nA in line #2, while control cells were electrically silent (Fig. 2 and fig. S3). During 10-s BL pulses, *Gt*ACR1 inactivated to 19 and 29% of the peak activity in line #1 (SD = 8, $n = 11$) and line #2 (SD = 14, $n = 10$), respectively (Fig. 2 and fig. S3). Apparently, *Gt*ACR1 functions as a bona fide light-gated ion channel that can conduct inward currents with peak amplitudes as high as −1 to −2 nA at −100 mV in tobacco guard cells.

*Gt*ACR1 thus can be used as a substitute for endogenous anion channels in guard cells, but the expression of these algal channels may feedback on the activity of the endogenous channels. To test this possibility, we used short (4 s) hyperpolarizing voltage pulses from −100 to −260 mV, which cause a temporal elevation of the cytosolic-free Ca^{2+} concentration that, in turn, activates S-type anion channels (*33*–*35*). No difference was found with respect to the average endogenous currents evoked by these voltage pulses between *Gt*ACR1-expressing guard cells (line #1; Fig. 3, A and C) and the control (Fig. 3, B and C). BL pulses of 0.1 s evoked additional anion currents in guard cells that expressed *Gt*ACR1 (line #1), with the same magnitude before, during, and after the period in which S-type anion channels were activated (Fig. 3D). These guard cell responses strongly suggests that *Gt*ACR1 and S-type anion channels do not mutually influence each other's activity. This conclusion is also supported by our observation that the expression of *Gt*ACR1 altered neither the activation of S-type anion channels by ABA (fig. S4) nor the velocity by which stomata opened in red light and closed in darkness (fig. S5). Apparently, the expression of *Gt*ACR1 channels does not disrupt the ability of cytosolic Ca^{2+} signals, ABA, and light to regulate the guard cell endogenous SLAC1-type anion channels (*23*).

During stomatal opening, guard cells can accumulate chloride, nitrate, and malate (*36*, *37*). Are these anions released by guard cells following *Gt*ACR1 activation? To answer this question, guard cells in isolated epidermal peels were stimulated with BL pulses (470 nm, 0.1 s, and 17 mW mm^{-2}), which were applied during a voltage ramp

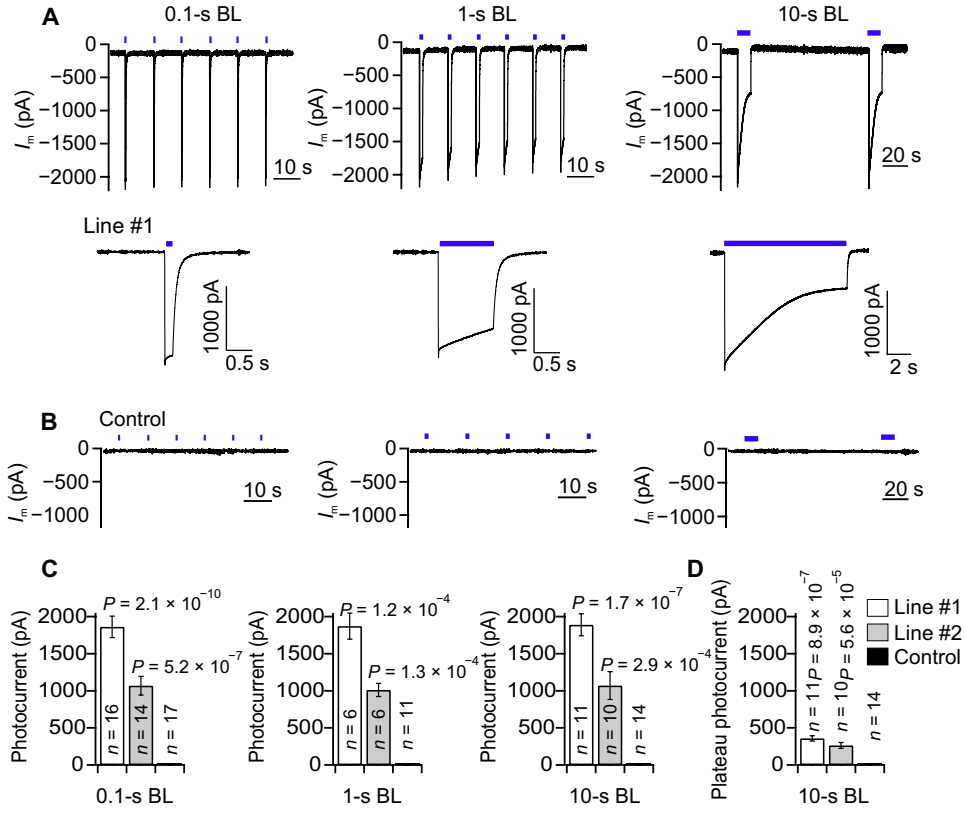

Fig. 2. *Gt*ACR1 photocurrents elicited by BL pulses in tobacco guard cells. (**A** and **B**) Current traces of guard cells in intact *Gt*ACR1 transformed plants (line #1) (A) and control plants (B) clamped to a V_m of −100 mV. The cells were stimulated with a train of BL pulses (blue bars above the traces, λ = 470 nm, 17 mW/mm^2), with a duration of 0.1 s (left), 1 s (middle), and 10 s (right). (A) Bottom: Expanded traces of single photocurrents triggered by BL pulses of 0.1, 1, or 10 s. (**C**) Mean amplitudes of peak photocurrents in guard cells of line #1, line #2, and control plants induced by BL pulses, with a duration as indicated below the graphs. (**D**) Plateau level of photocurrents determined at the end of the 10-s BL pulses [as shown in (A), bottom left] for guard cells of line #1, line #2, and control plants. In (C) and (D), the *P* values were determined with a Student's *t* test using values of *Gt*ACR1 line #1 or #2 and control plants; the number of experiments is given in the respective bars, and error bars represent SE.

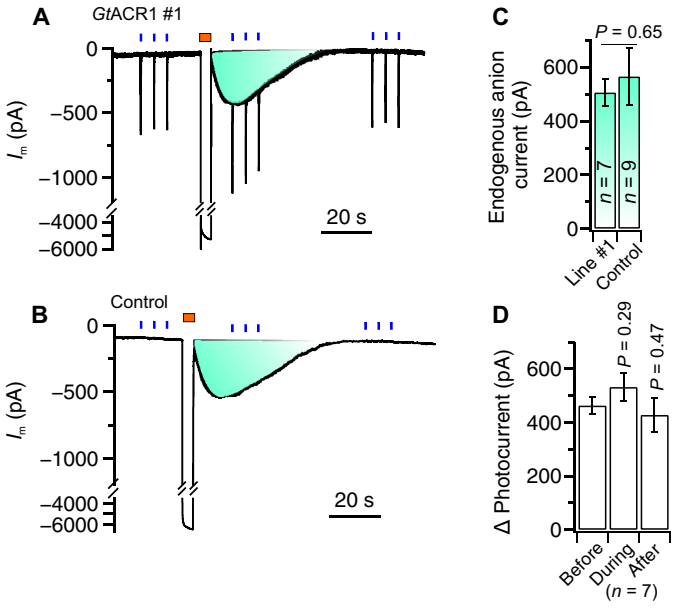

Fig. 3. *Gt*ACR1 photocurrents are additive to endogenous SLAC-type anion currents. (**A** and **B**) Traces of plasma membrane current measured for guard cells that were clamped to a membrane potential of −100 mV. The cells were stimulated three times with three successive BL pulses of 0.1 s (0.06 mW/mm^2) (indicated by blue bars above the traces) and a 4-s hyperpolarizing pulse from a potential of −100 to −260 mV (indicated by a brown bar above the traces). Note that the BL pulses evoked currents of approximately −500 pA in *Gt*ACR1-expressing guard cells [(A) line #1], which were additive to the transient current induced by the voltage pulse. In control cells (B), BL did not provoke changes in plasma membrane current, but the peak current induced by voltages pulses was the same in *Gt*ACR1 line #1 and control cells (**C**). (**D**) Average of photocurrents in guard cells of *Gt*ACR1 line #1, determined before, during, and after the activation of endogenous anion channels with a voltage pulse.

from −100 to 65 mV (Fig. 4A). At an extracellular Cl^- concentration of 99 mM, the reversal potential of *Gt*ACR1 was −2 mV (SE = 8, n = 5), while it shifted to 55 mV when guard cells were transferred to 3 mM Cl^- (Fig. 4, B and C). As with Cl^-, a change of the NO_3^- concentration from 99 to 3 mM caused a shift of the reversal potential by 50 mV (Fig. 4, D and E). The reversal potential of *Gt*ACR1 thus displays a similar sensitivity to changes in the Cl^- and NO_3^- concentration, indicating that the light-activated channel is permeable to both monovalent anions same as the guard cell intrinsic ABA-activated anion channel SLAC1 (*38*).

The divalent organic anion malate^{2-} and SO_4^{2-} represent major substrates of QUAC1 (quick anion channel 1)/R-type guard cell anion channels (*36*, *39*–*41*). However, neither the application of malate^{2-} nor that of SO_4^{2-} altered the *Gt*ACR1 reversal potential (fig. S6). We thus conclude that *Gt*ACR1 only conducts monovalent anions (*20*), which is a key feature of SLAC1 in guard cells.

Guard cell *Gt*ACR1 activity depends on light intensity and quality

It is possible that the properties of light-gated channels are affected by the cells that express the optogenetic tool in question. We thus tested the dependency of *Gt*ACR1 on the light intensity and wavelength in tobacco guard cells. The light intensity of three sequential 0.1-s BL pulses (470 nm) was stepwise increased from 0.06 to 17 mW mm^{-2} (Fig. 5A and fig. S7A). The membrane current increased with a rise in light intensity and saturated (>0.95 of maximal value) at 7.8 mW mm^{-2} in line #1 (Fig. 5, A and B). On average, the currents in line #1 reached their half-maximum value at 0.41 mW mm^{-2} (SE = 0.16, n = 6), a value that is two to five times higher than that determined for *Gt*ACR1 in human embryonic kidney cells (*20*). We also searched for light qualities, other than BL, which can activate *Gt*ACR1 in tobacco. Guard cells were stimulated with three sequential high-intensity (equivalent photon flux density as BL at 17 mW mm^{-2}) light flashes of 0.1 s, of which the wavelength was varied from violet (405 nm) to red (660 nm) (Fig. 5C and fig. S7B). Light pulses with wavelengths ranging from 405 to 580 nm evoked large plasma membrane currents, but the response decreased at wavelengths above 595 nm, and only minor currents were detected at 660 nm (Fig. 5, C and D). These data thus show that *Gt*ACR1 is also highly sensitive to green light, which is hardly absorbed by chloroplasts and therefore does not interfere with photosynthesis.

Prolonged *Gt*ACR1 stimulation activates guard cell K^+ efflux channels and H^+ pumps

The anion currents through *Gt*ACR1 trigger a depolarization, which is likely to provoke the activation of K^+ efflux channels in the guard cell plasma membrane (*28*, *42*) and/or activation of voltage-dependent H^+-pumps (*14*). We tested the potential contribution of K^+ channels and H^+ pumps to the *Gt*ACR1-evoked E_m response by iontophoretic loading of inhibitors via intracellular double-barreled microelectrodes. K^+ efflux channels in tobacco guard cells are most likely encoded by *Nt*GORK (fig. S1) and can be blocked with intracellular Cs^+ (*43*). This prevented repolarization of E_m after termination of the light stimulus (Fig. 6, A and B, and fig. S8) and strongly delayed E_m recovery (Fig. 6, B and D). The voltage-dependent activation of *Nt*GORK thus appears to counteract the depolarization evoked by *Gt*ACR1 in guard cells.

Guard cells are energized by H^+-ATPases that generate a proton motive force and cause hyperpolarization of E_m (*44*, *45*). The activity of these pumps was inhibited by iontophoretic loading of orthovanadate. The initial BL response, marked by a fast depolarization and repolarization, was not affected by vanadate (Fig. 6, A and C). However, instead of a slow recovery of E_m after this initial response, a second depolarization phase was observed for vanadate-treated cells (Fig. 6, A and C), which was followed by a very slow recovery of E_m after termination of the BL pulse (Fig. 6, A, C, and D). The second depolarization was observed in 9 of 14 cells of line #1 and 4 of 5 cells of line #2 and may be linked to a cytosolic acidification of vanadate-loaded guard cells, which leads to inhibition of GORK-like channels (*28*, *46*, *47*). In control cells, cytosolic acidification will be counteracted by the active H^+-ATPases, and this will prevent a prolonged depolarization during BL stimulation of *Gt*ACR1.

The impact of the successive activation of K^+ efflux channels and the H^+-ATPase on the *Gt*ACR1-induced depolarization was studied with a mathematical model. Models for guard cells responses have been published earlier (*48*, *49*), but these models were based on holistic approaches and therefore not suitable for our purpose. We developed the minimal GuardIon model (Fig. 6E and fig. S9), in which the ensemble of conductance changes simulated the recorded membrane potential changes with high accuracy (Fig. 6, A and E). Starting from the resting state, the BL activation of *Gt*ACR1 resulted in a depolarization that caused mainly the activation of GORK, which, in turn, provoked a first repolarization. After the light pulse,

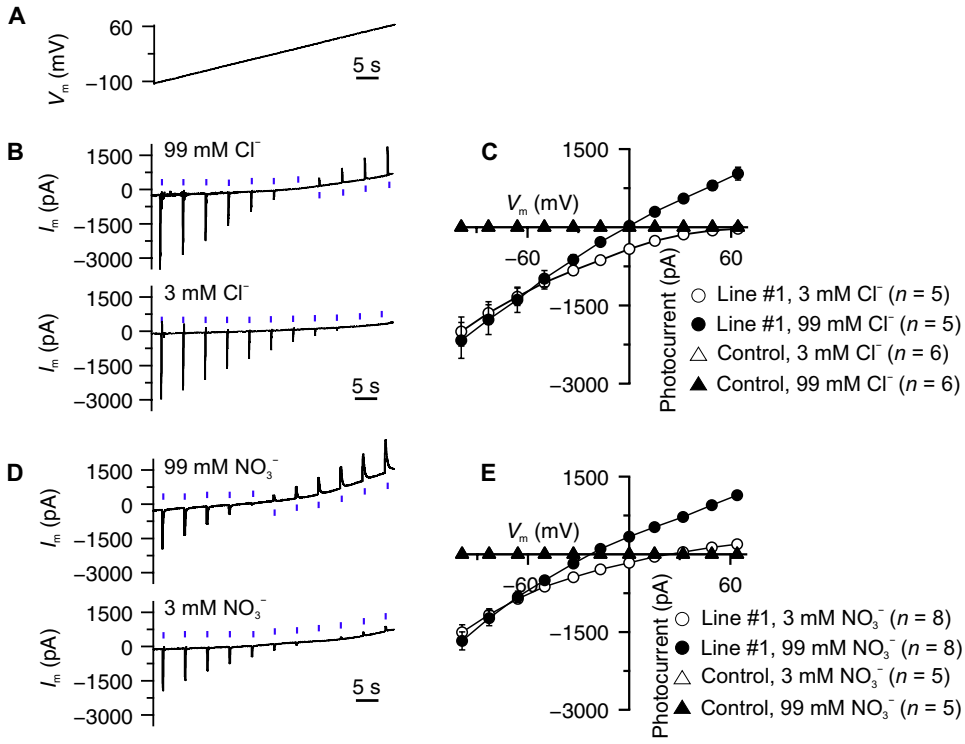

Fig. 4. Anion selectivity of *Gt*ACR1 in tobacco guard cells. (**A**) Voltage ramp applied to guard cells, to determine the reversal potential of *Gt*ACR1. (**B** and **D**) Photocurrents of *Gt*ACR1 in guard cells of line #1, clamped to a voltage ramp from −100 to 65 mV, as indicated in (A) and stimulated with BL pulses of 0.1 s, every 5 s. The guard cells in epidermal strips were measured in bath solutions containing monovalent anions at the concentration indicated above the traces. (**C** and **E**) Average peak photocurrents plotted against the clamp potential for cells bathed in Cl^- (C) and NO_3^- (E) at two concentrations, as indicated in the graphs.

the membrane voltage returned quickly to the resting state. Thus, the main actors during the light pulse were *Gt*ACR1 and the K^+ efflux channel, while the other transporters only had a minor impact (Fig. 6, E and F).

Long-term activation of *Gt*ACR1 triggers K^+ efflux and stomatal closure

*Gt*ACR1-mediated anion currents might be sufficient to trigger stomatal closure, given that this response would enable a simultaneous efflux of K^+ (*6*, *7*, *9*). During a strong depolarization caused by the activation of *Gt*ACR1 (Fig. 1), guard cells should activate *Nt*GORK (Fig. 6, E and F) and thus may provide for long-term extrusion of K^+. We tested this hypothesis with the scanning ion-selective electrode (SISE) technique (*50*). Activation of *Gt*ACR1 with BL caused the efflux of K^+ from line #1 (Fig. 7A) and line #2 (fig. S10), while no K^+ extrusion was found with control stomata (Fig. 7A).

When applying long-lasting light pulses in computational simulations, the GuardIon model predicted that simultaneous long-term extrusion of anions through *Gt*ACR1 and K^+ via GORK provoked a reduction in guard cell osmotic pressure (Fig. 7B; see fig. S9 for details), which is likely to close the stomatal pore. The speed by which guard cells lose turgor depends on the conductance of *Gt*ACR1. While an effective steady-state conductance, i.e., the current that remains after inactivation (30% of the peak value), of 1500 pS provoked a complete loss of guard cell turgor in approximately 15 min, lowering the conductance extended this period (Fig. 7B).

We provoked stomatal closure in tobacco leaves with continuous green light (λ = 525 nm, 0.57 mW/mm^2), as this light quality activates *Gt*ACR1 but hardly affects photosynthesis. This light stimulus was projected via the objective on a small leaf area (2×10^3 µm^2) and induced an average steady-state current of −75 pA in line #1 (fig. S11), which is equivalent to a plasma membrane conductance of around 500 pS. Stomata in intact leaves started to close soon after onset of green light, and the speed of stomatal closure accelerated thereafter (Fig. 7C). The slight differences between the predicted changes in turgor pressure (Fig. 7B) and stomatal aperture (Fig. 7C) are probably due to a nonlinear relation between these two parameters (*51*).

The optogenetic experiments with individual stomata (Fig. 7, C and D) showed that activation of *Gt*ACR1 by green light provoked stomatal closure. However, can we also control transpiration if an entire population of *Gt*ACR1-expressing stomata is stimulated with green light? To answer this question, intact tobacco leaves were studied with a custom-made gas exchange system (*52*), in which the stomata of all three lines opened upon illumination with red light (650 nm) (Fig. 7E). Stimulation of the whole leaf with green light (520 nm) caused a reduction of the transpiration in lines #1 and #2, while the stomata of control leaves opened further (Fig. 7E). The expression of *Gt*ACR1 thus provides a noninvasive tool, which can reverse the direction of stomatal movements in intact plants.

DISCUSSION

Activation of the light-gated anion channel *Gt*ACR1, in the plasma membrane of tobacco guard cells, is sufficient to provoke rapid stomatal closure (Fig. 7, C to E). This shows that *Gt*ACR1 functions as

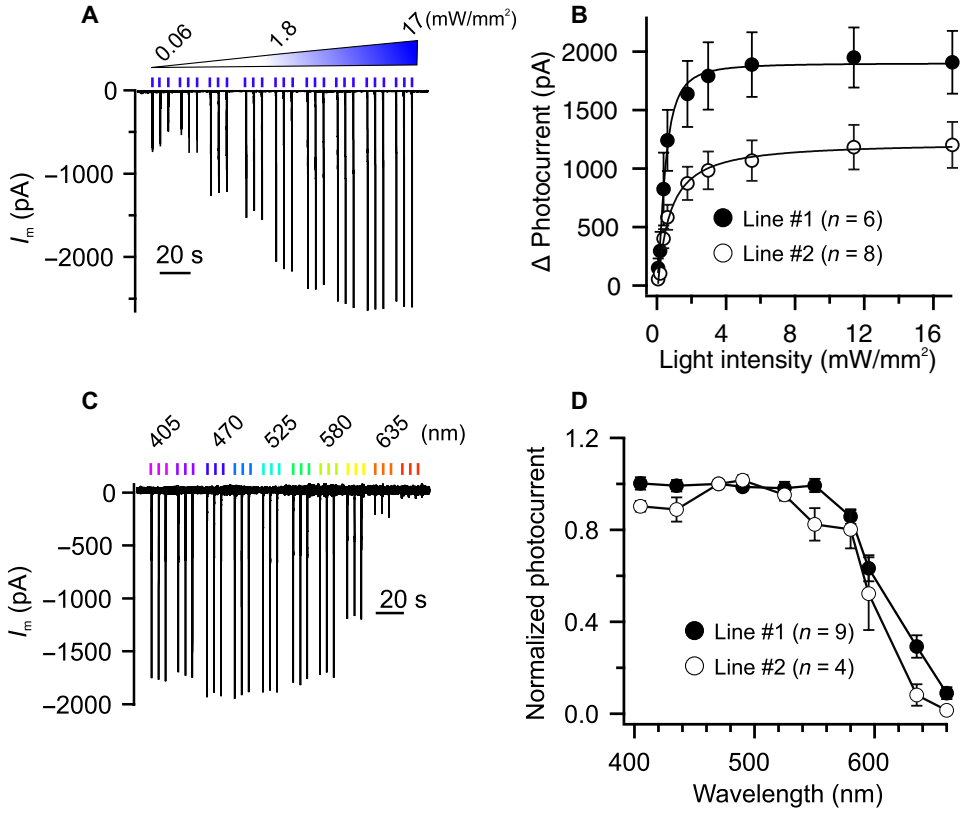

Fig. 5. Photoactivity of *Gt*ACR1 in tobacco guard cells. (**A** and **B**) Impact of light-intensity on photocurrents in guard cells of line #1. (A) Current trace of a guard cell (line #1) clamped to −100 mV and stimulated with three successive BL pulses of 0.1 s of which the light intensity ranged from 0.06 to 17 mW mm^{-2}. (B) Peak photocurrents plotted against the intensity of the BL pulses. The photocurrents were fitted with a Michaelis-Menten function (solid lines), which revealed half-maximal values of 0.42 ± 0.16 and 0.86 ± 0.27 mW mm^{-2} for *Gt*ACR1 in lines #1 and #2, respectively. (**C** and **D**) Wavelength dependence of *Gt*ACR1 expressed in tobacco guard cells. (C) Current trace of a guard cell (line #1) that was clamped to −100 mV and stimulated with three successive light pulses (equivalent photon flux density as BL at 17 mW mm^{-2}) with wavelengths ranging from 405 to 660 nm (as indicated above the current trace). (D) Average peak photocurrents elicited with light pulses (17 mW mm^{-2}) in guard cells (line #1 and #2), clamped to −100 mV, and plotted against the wavelength of the light pulses.

a stand-in for endogenous guard cell anion channels. While *Gt*ACR1 is activated by simple light signals, the natural guard cell anion channels are regulated by complex pathways that are activated by ABA and CO_2, as well as microbial factors (*43*, *53*–*57*). The stress hormone ABA was also shown to regulate the activity of plasma membrane K^+ channels (*46*, *58*), Ca^{2+}-permeable channels (*59*, *60*), and the H^+-ATPase (*61*, *62*). Our data now indicate that the latter responses are not strictly required to provoke stomatal closure.

Our data obtained with *Gt*ACR1 and the GuardIon model indicate that closure of the stomatal pore primarily depends on the activity of anion channels. These channels provoke the depolarization of guard cells, which activates GORK-like K^+ efflux channels and leads to a simultaneous efflux of anions and K^+ (*2*, *23*). How can we get further insights into the molecular mechanisms of this early stomatal closure phase?

Previous studies have suggested that ABA, CO_2, and microbial factors address anion and K^+ channels through signaling pathways that involve Ca^{2+} and pH signals (*8*, *9*, *18*, *63*, *64*). Are these second messengers required for the coordination of ion transport in guard cells to speed up stomatal closure (*35*)? With the light-activated, proton-permeable channel ChR2-XXL (*14*) and the calcium-permeable channel ChR2-XXM (*65*), new tools have become available to address these long-standing questions. This toolbox—which also includes BLINK1 (*13*), *Gt*ACR1 (*15*), and other anion channelrhodopsins (*66*)—will be very valuable in assigning the relative functions of voltage, pH, and Ca^{2+} signals in the regulation of stomatal movements.

The occurrence of patchy stomatal conductance is a poorly understood and mostly neglected phenomenon (*67*, *68*). The difficulty of studying this phenomenon is its rather unpredictable appearance. The use of channelrhodopins, in combination with structured illumination of leaves, may change this situation, as we can now provoke stomatal patchiness and analyze its impact on water use efficiency.

In addition, optogenetic tools can be key to tackle other long-standing questions in plant biology. One of these outstanding questions is the nature and role of long-distance signals in plants, which are evoked by abiotic and biotic stress and travel along the phloem and/or xylem parenchyma (*69*, *70*). The rhodopsin-based toolbox is likely to bring new insights in the functions of these propagating voltage, pH, and Ca^{2+} signals. Moreover, the expression of light-gated Ca^{2+} permeable channels opens the unique possibility to impose Ca^{2+} signatures, with unique amplitude or frequency, and test how these Ca^{2+} signals trigger specific responses in plant cells (*71*).

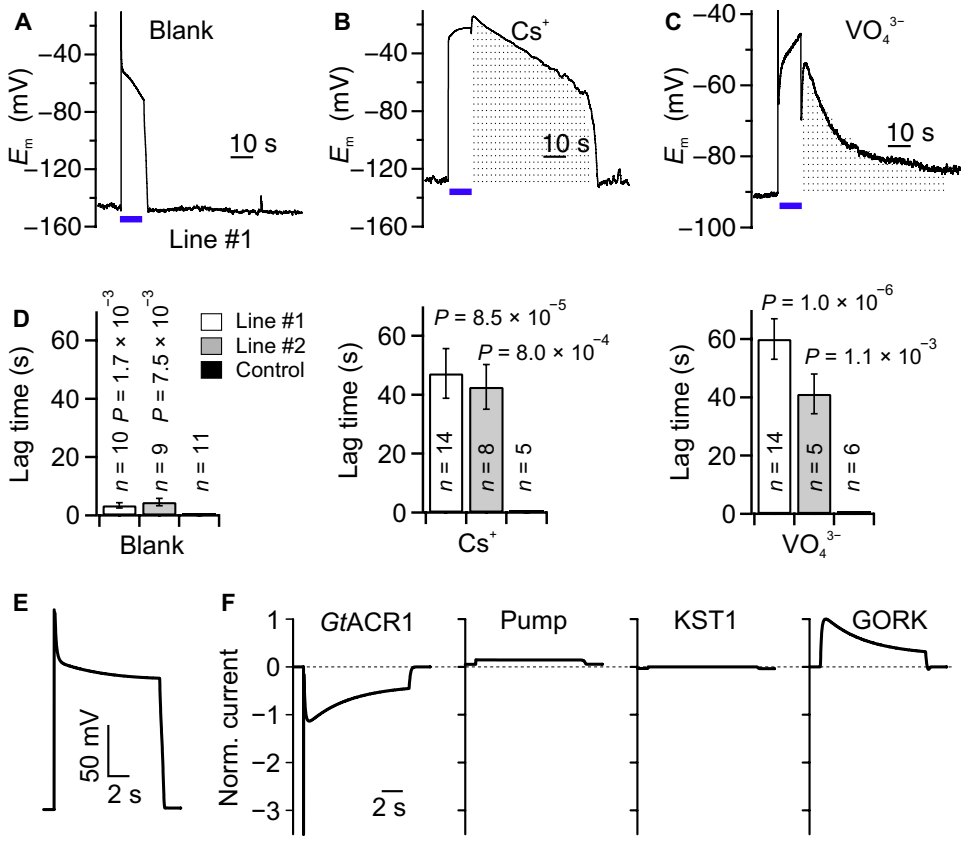

Fig. 6. Impact of K^+ efflux channels and H^+-ATPases on *Gt*ACR1-induced responses of guard cells. (**A** and **C**) Membrane potential traces of tobacco guard cells of line #1. The cells were studied with electrodes that contained only KCl (A) and were loaded with Cs^+ (**B**) or VO_4^{3-} (C). A BL pulse of 10 s (as indicated by the bars below the traces) was used to stimulate the cells. The gray dotted area indicates the difference in responses between the blank (A) and Cs^+-treated (B) or VO_4^{3-}-treated (C) cells. (**D**) Average lag time between termination of the BL pulse and full recovery of E_m in guard cells of line #1, line #2, and control plants in experiments with KCl-containing electrodes or after treatment with Cs^+ and VO_4^{3-}. *P* values were determined with a Student's *t* test using values of *Gt*ACR1 line #1 or #2 and control plants. The number of experiments is given in the respective bars, and error bars represent SE. (**E** and **F**) Computational simulation with the GuardIon model. Initially, the model guard cell is at rest, and after 0.5 s, a light pulse activates *Gt*ACR1 [left panel in (F)], which induces a depolarization (E) and, in response, activates the pump [second panel in (F)] and GORK [right panel in (F)] while it deactivates KST1 [third panel in (F)]. Because of the activation of GORK, the cell rapidly repolarizes during stimulation with BL (E), while a full recovery occurs when *Gt*ACR1 is no longer activated with BL.

MATERIALS AND METHODS

Plant growth conditions

The UBQ10::Ret-ACR1 2.0 and UBQ10::Ret-eYFP transgenic tobacco (*Nicotiana tabacum*) plants used in this study were in the SR1 background and described earlier (*15*). Seeds were sown on sterilized soil, and plants were grown in a climate cabinet, illuminated with red light-emitting diodes (LEDs; peak intensity at 650 nm and photon flux density of 100 µmol m^{-2} s^{-1}), at a day/night photoperiod of 12/12 hours, with the temperature cycling between 22° and 18°C and a relative air humidity of 60%. After 2 weeks, the seedlings were carefully transferred to new pots (diameter of 6 cm) and grown for another 2 to 3 weeks at the same conditions. Because of activation of *Gt*ACR1 at wavelengths of ≤620 nM (Fig. 5D), cultivation of *Gt*ACR1-expressing plants and the controls occurred with red light as the sole source of photosynthetic active radiation (*15*).

Electrophysiological recording in intact plants

For electrophysiological recordings on guard cells, the adaxial side of the second leaf of intact plants was gently fixed to a plexiglass holder using a double-sided adhesive tape. The plexiglass holder with leaf was then placed in the focal plane of an upright microscope (Akioskop 2FS, Zeiss, Germany). The leaves were illuminated with red light (0.018 mW/mm^2), which was provided by a halogen bulb in the microscope lamp, and filtered through a red-light glass filter (cutoff wavelength of 635 nm). A drop of bath solution [1 mM KCl, 1 mM $CaCl_2$, and 10 mM MES (2-(N-morpholino)ethanesulfonic acid)/BTP (Bis-tris propane) (pH 6)] was placed between the objective (W Plan-Apochromat, 63×/1.0, Zeiss) and the leaf surface. A capillary filled with 300 mM KCl and sealed with 2% agarose in 300 mM KCl served as a reference electrode and was placed with one side in the bath solution, while the other end was connected to the ground via an AgCl/Cl half-cell. In this experimental configuration, guard cells in the abaxial side of the leaf were accessible for impalement with double-barreled microelectrodes. All microelectrodes were fabricated from borosilicate glass capillaries (inner/outer diameter = 0.56/1.0 mm; Hilgenberg, Germany), which were aligned, heated, twisted 360°, prepulled by a vertical puller (L/M-3P-A, Heka, Germany), and subsequently pulled on a horizontal laser puller (P2000, Sutter Instruments, CA, USA). The double-barreled microelectrodes were filled with 300 mM KCl and had a resistance ranging between

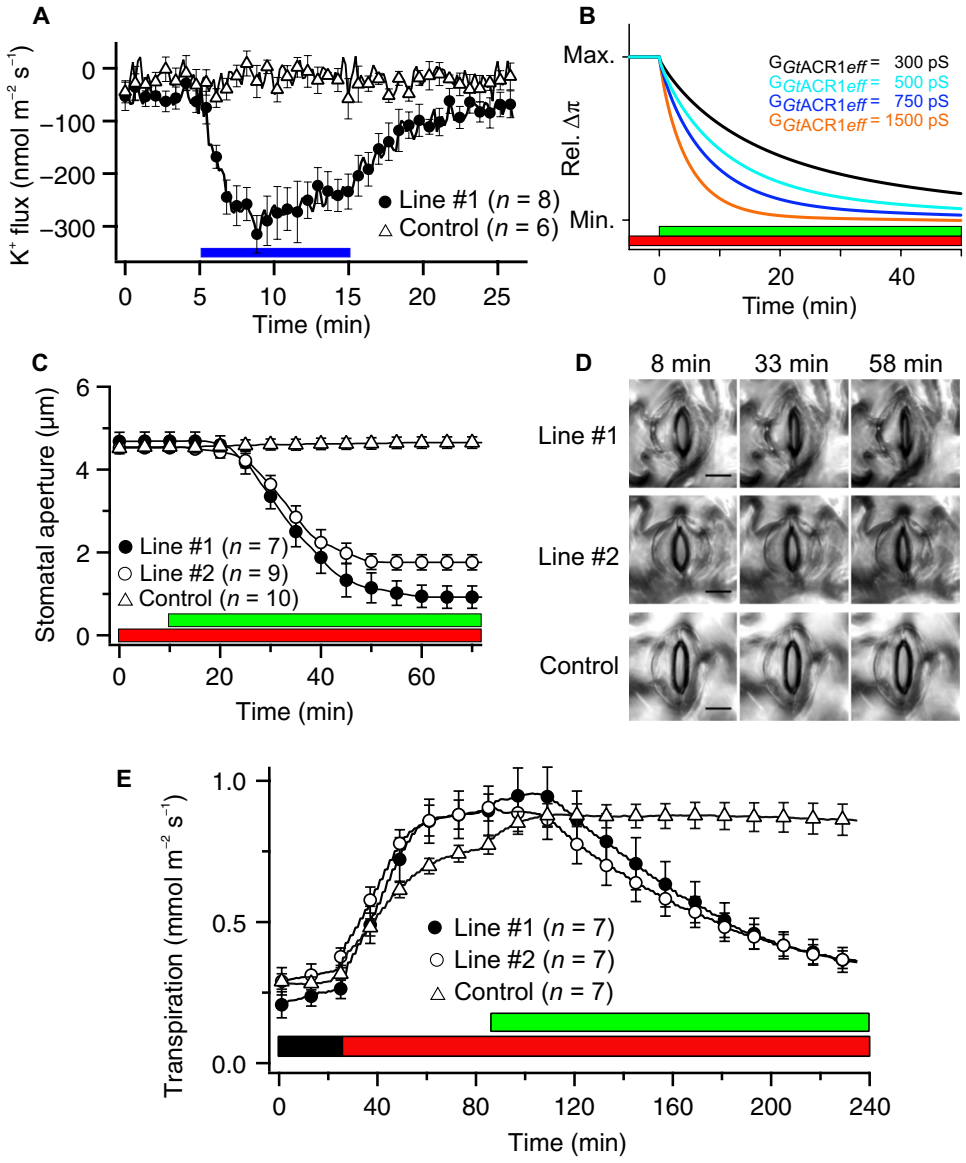

Fig. 7. *Gt*ACR1 enables light-controlled stomatal closure. (**A**) Average values of K^+ flux of tobacco guard cells in epidermal peels, which were stimulated with a 10-min BL pulse (0.15 mW/mm^2). The SISE technique was used to determine K^+ efflux from guard cells of line #1 (solid circle) and control plants (open triangle). Error bars represent SE. (**B**) Osmotic pressure difference across the plasma membrane predicted by the Guardlon model. (**C** and **D**) Light-controlled stomatal closure in *Gt*ACR1-expressing lines (#1 and #2) and control plants. (**C**) The aperture of stomata in intact plants was first monitored in red light only (λ = 630 nm, 0.018 mW/mm^2), and thereafter, additional green light was provided (λ = 525 nm, 0.57 mW/mm^2), as indicated by the bars below the graph. (**D**) Representative images of stomata before stimulation with green light (8 min) and during green light stimulation (33 and 58 min) are shown of lines #1, #2, and control plants. Scale bars, 15 µm. See also movie S1. (**E**) Transpiration of tobacco leaves, as measured in gas exchange setup, in darkness, during illumination with red light only (λ = 650 nm, 0.067 mW/mm^2), and after addition of green light (λ = 520 nm, 0.017 mW/mm^2), as indicated by the bars below the traces. Error bars represent SE (n = 7).

130 to 170 megohm. Guard cells were impaled with a piezo-driven micromanipulator (MM3A, Kleindiek, Reutlingen, Germany). The microelectrodes were connected to headstages with an input impedance of 100 gigohm via Ag/AgCl half-cells. A custom-made amplifier (Ulliclamp01) was connected to the headstages, and electrical signals were low pass–filtered at 0.5 kHz with a dual low-pass Bessel filter (LPF 202A; Warner Instruments Corp., USA) and recorded at 1 kHz with an interface (USB-6002, NI, USA) that was controlled by WinWCP software (*72*).

Light stimulation and monitoring of stomatal movements

Guard cells were stimulated with light pulses guided through the W Plan-Apochromat objective (63×/1.0, Zeiss). The light pulses were provided by an LED illumination system (pE-4000, CoolLED, UK), in which most of the visible spectrum is covered by 16 LEDs. The illumination system was connected to a CARV II confocal spinning disc unit (Crest Optics, Rome, Italy) that was mounted on the microscope. Light was reflected by either a gray mirror or dichroic mirrors in the CARV unit through the objective at the specimen.

The duration, time interval, and intensity of light pulses were controlled by the VisiView software (Visitron, Puchheim, Germany), and the same software was used to follow stomatal movements using a charge multiplying charge-coupled device camera (QuantEM, Photometrics, USA). Images were processed with ImageJ in the Fiji software package (*73*). The light intensity applied via a 63× objective was determined with a quantum sensor (Q13627, LI-COR, USA) connected to a light meter (LI-COR, Model LI-189). The measured quantum flux data were corrected for the illuminated area and converted into light intensity values.

Ion selectivity measurements

The ion selectivity measurements were carried out with guard cells in isolated epidermal peels, which were obtained from the second leaf of 4-week-old plants, and gently fixed on microscope slides with Medical Adhesive B (Aromando, Düsseldorf, Germany). The strips were incubated in a bath solution [0.1 mM $CaCl_2$ and 10 mM Mes/BTP (pH 6.0)] supplemented with 3 mM KCl, 3 mM KNO_3, 1.5 mM K_2SO_4, or 1.5 mM K_2malate (pH 6) for at least 2 hours before the start of measurements. Thereafter, the microscope slides with epidermal peels were transferred to a measuring chamber with 500 µl of bath solution. Guard cells were impaled with double-barreled electrodes filled with 300 mM CsCl and clamped at −100 mV. During a voltage ramp protocol from −140 to +60 mV (3 mV s^{-1}), a series of light pulses (0.1-s BL of 470 nm at 5-s intervals) were applied. After the first measurement, the bath solution was exchanged with one that was supplemented with 99 mM KCl, 99 mM KNO_3, 50 mM K_2SO_4, or 50 mM K_2malate (pH 6), respectively, and the voltage-clamp measurement was repeated.

Noninvasive ion flux measurements

K^+ fluxes across the plasma membrane of guard cells were monitored in isolated epidermal strips with the noninvasive SISEs, as described in (*50*). Epidermal strips from the abaxial side of tobacco leaves were gently peeled and glued to microscope slides with Medical Adhesive B. The microscope slides were immediately transferred to the measuring chamber and filled with 1.5 ml of bath solution [0.1 mM KCl, 0.1 mM $CaCl_2$, and 0.1 mM MES/BTP (pH 6)]. The strips were kept in the bath solution for 1 to 2 hours in the dark before the SISE recordings were started. The electrodes for ion flux measurements were pulled from borosilicate glass capillaries without filaments (Ø of 1.0 mm; Science Products, Hofheim, Germany) on a vertical puller (Narishige, Tokyo, Japan). The electrodes were baked over night at 220°C, silanized with *N*,*N*-dimethyltrimethylsilylamine (Sigma-Aldrich), and kept at 220°C for another hour. The electrodes were first filled with backfill solution (1 mM KCl) and thereafter tip-filled with the potassium ionophore I cocktail B (Sigma-Aldrich). Before the experiments, the electrodes were calibrated in solutions with 0.1, 1, and 10 mM KCl, and only electrodes that showed a shift of 58 mV per pK unit were used for measurements. The electrode was connected to the headstage of the microelectrode amplifier (custom-built) via Ag/AgCl half-cells and positioned at approximately 5-µm distance of a stoma with a micromanipulator (PatchStar, Scientifica, Uckfield, UK). The electrodes were moved over a distance of 50 µm, at an angle of 45° to the epidermal strip, at 10-s intervals. Raw data were acquired with a NI interface (USB 6002) using a custom-built Labview-based software "Ion Flux Monitor." Raw voltage data were converted offline with the Ion Flux Analyzer program into ion flux data as described (*74*, *75*).

Confocal microscopy and image processing

The fluorescent signal of *Gt*ACR1-eYFP or soluble eYFP was detected with a confocal laser scanning microscope (Leica SP5, Leica Microsystems CMS, Mannheim, Germany). eYFP was excited with light of 496 nm, and the fluorescence was captured between 520 to 580 nm using a dipping 25× HCX IRAPO 925/0.95 objective. The ImageJ software was used for image processing.

Quantitative real-time polymerase chain reaction

Quantification of *Gt*ACR1, *Nt*FAMA1, *Nt*KST1, *Nt*GORK, and *Nt*SLAC1 transcripts was performed by quantitative polymerase chain reaction (PCR) as described elsewhere (*76*). Leaves of 5-week-old *N. tabacum* plants were harvested for reverse transcription PCR analysis. Guard cells were mechanically isolated (*24*); major veins were removed, and leaf blades from two young plants were fractionated in a blender with a mixture of ice and deionized water, twice for 1 to 2 min. Guard cells samples were collected on a 210-nm nylon mesh for subsequent RNA extraction. As a reference, RNA was extracted from leaves of which the abaxial epidermis was removed. The transcript level of each gene was determined relative to that of 10,000 molecules of actin. The primers used to quantify transcript levels are listed in table S1.

Gas exchange measurements

Leaf transpiration was measured with a custom-made system, which was described previously (*52*), using 4- to 5-week-old intact tobacco plants, at 20°C, 50% relative humidity, and 400 parts per million of CO_2. Evaporation of water from the soil was prevented by sealing the whole pots with plastic wrap. Before the measurement, the plants were kept in darkness until the transpiration rate had stabilized, at least for 1 hour. Subsequently, plants were illuminated with red light (67 µW/mm^2, 650 nm), and after 1 hour, additional green light (17 µW/mm^2, 520 nm) was applied or the red light was switched off.

The GuardIon model

The essential players for the observed ion fluxes were identified, and their features were described mathematically, and computational cell biological simulations were carried out as outlined in detail in the Supplementary Materials.

SUPPLEMENTARY MATERIALS

Supplementary material for this article is available at http://advances.sciencemag.org/cgi/content/full/7/28/eabg4619/DC1

View/request a protocol for this paper from *Bio-protocol*.

REFERENCES AND NOTES

1. S. Jasechko, Z. D. Sharp, J. J. Gibson, S. J. Birks, Y. Yi, P. J. Fawcett, Terrestrial water fluxes dominated by transpiration. *Nature* **496**, 347–350 (2013).
2. H. Kollist, M. Nuhkat, M. R. G. Roelfsema, Closing gaps: Linking elements that control stomatal movement. *New Phytol.* **203**, 44–62 (2014).
3. T. J. Brodribb, F. Sussmilch, S. A. M. McAdam, From reproduction to production, stomata are the master regulators. *Plant J.* **101**, 756–767 (2020).
4. E. Marris, Water: More crop per drop. *Nature* **452**, 273–277 (2008).
5. P. J. Franks, J. A. Berry, D. L. Lombardozzi, G. B. Bonan, Stomatal function across temporal and spatial scales: Deep-time trends, land-atmosphere coupling and global models. *Plant Physiol.* **174**, 583–602 (2017).
6. K. Raschke, R. Hedrich, U. Reckmann, J. I. Schroeder, Exploring biophysical and biochemical-components of the osmotic motor that drives stomatal movement. *Bot. Acta* **101**, 283–294 (1988).
7. M. R. G. Roelfsema, R. Hedrich, In the light of stomatal opening: New insights into 'the Watergate'. *New Phytol.* **167**, 665–691 (2005).

8. T.-H. Kim, M. Böhmer, H. H. Hu, N. Nishimura, J. I. Schroeder, Guard cell signal transduction network: Advances in understanding abscisic acid, CO_2, and Ca^{2+} signaling. *Annu. Rev. Plant Biol.* **61**, 561–591 (2010).
9. M. Jezek, M. R. Blatt, The membrane transport system of the guard cell and its integration for stomatal dynamics. *Plant Physiol.* **174**, 487–519 (2017).
10. A. Adamantidis, S. Arber, J. S. Bains, E. Bamberg, A. Bonci, G. Buzsáki, J. A. Cardin, R. M. Costa, Y. Dan, Y. Goda, A. M. Graybiel, M. Häusser, P. Hegemann, J. R. Huguenard, T. R. Insel, P. H. Janak, D. Johnston, S. A. Josselyn, C. Koch, A. C. Kreitzer, C. Lüscher, R. C. Malenka, G. Miesenböck, G. Nagel, B. Roska, M. J. Schnitzer, K. V. Shenoy, I. Soltesz, S. M. Sternson, R. W. Tsien, R. Y. Tsien, G. G. Turrigiano, K. M. Tye, R. I. Wilson, Optogenetics: 10 years after ChR2 in neurons-views from the community. *Nat. Neurosci.* **18**, 1202–1212 (2015).
11. B. R. Rost, F. Schneider-Warme, D. Schmitz, P. Hegemann, Optogenetic tools for subcellular applications in neuroscience. *Neuron* **96**, 572–603 (2017).
12. S. Beck, J. Yu-Strzelczyk, D. Pauls, O. M. Constantin, C. E. Gee, N. Ehmann, R. J. Kittel, G. Nagel, S. Gao, Synthetic light-activated ion channels for optogenetic activation and inhibition. *Front. Neurosci.* **12**, 643 (2018).
13. M. Papanatsiou, J. Petersen, L. Henderson, Y. Wang, J. M. Christie, M. R. Blatt, Optogenetic manipulation of stomatal kinetics improves carbon assimilation, water use, and growth. *Science* **363**, 1456–1459 (2019).
14. A. Reyer, M. Häßler, S. Scherzer, S. Huang, J. T. Pedersen, K. A. S. Al-Rascheid, E. Bamberg, M. G. Palmgren, I. Dreyer, G. Nagel, R. Hedrich, D. Becker, Channelrhodopsin-mediated optogenetics highlights a central role of depolarization-dependent plant proton pumps. *Proc. Natl. Acad. Sci. U.S.A.* **117**, 20920–20925 (2020).
15. Y. Zhou, M. Q. Ding, S. Q. Gao, J. Yu-Strzelczyk, M. Krischke, X. D. Duan, J. Leide, M. Riederer, M. J. Mueller, R. Hedrich, K. R. Konrad, G. Nagel, Optogenetic control of plant growth by a microbial rhodopsin. *Nat. Plants* **7**, 144–151 (2021).
16. T. Vahisalu, H. Kollist, Y. F. Wang, N. Nishimura, W. Y. Chan, G. Valerio, A. Lamminmaki, M. Brosche, H. Moldau, R. Desikan, J. I. Schroeder, J. Kangasjarvi, SLAC1 is required for plant guard cell S-type anion channel function in stomatal signalling. *Nature* **452**, 487–491 (2008).
17. J. Negi, O. Matsuda, T. Nagasawa, Y. Oba, H. Takahashi, M. Kawai-Yamada, H. Uchimiya, M. Hashimoto, K. Iba, CO_2 regulator SLAC1 and its homologues are essential for anion homeostasis in plant cells. *Nature* **452**, 483–486 (2008).
18. M. R. G. Roelfsema, R. Hedrich, D. Geiger, Anion channels: Master switches of stress responses. *Trends Plant Sci.* **17**, 221–229 (2012).
19. S. W. Xue, H. H. Hu, A. Ries, E. Merilo, H. Kollist, J. I. Schroeder, Central functions of bicarbonate in S-type anion channel activation and OST1 protein kinase in CO_2 signal transduction in guard cell. *EMBO J.* **30**, 1645–1658 (2011).
20. E. G. Govorunova, O. A. Sineshchekov, R. Janz, X. Q. Liu, J. L. Spudich, Natural light-gated anion channels: A family of microbial rhodopsins for advanced optogenetics. *Science* **349**, 647–650 (2015).
21. J. Wietek, M. Broser, B. S. Krause, P. Hegemann, Identification of a natural green light absorbing chloride conducting channelrhodopsin from *Proteomonas sulcata*. *J. Biol. Chem.* **291**, 4121–4127 (2016).
22. H. Barbier-Brygoo, A. De Angeli, S. Filleur, J. M. Frachisse, F. Gambale, S. Thomine, S. Wege, Anion channels/transporters in plants: From molecular bases to regulatory networks, in *Annual Review of Plant Biology, Vol 62,* S. S. Merchant, W. R. Briggs, D. Ort, Eds. (Annual Review of Plant Biology, Annual Reviews, Palo Alto, 2011), vol. 62, pp. 25–51.
23. R. Hedrich, D. Geiger, Biology of SLAC1-type anion channels - from nutrient uptake to stomatal closure. *New Phytol.* **216**, 46–61 (2017).
24. H. Bauer, P. Ache, S. Lautner, J. Fromm, W. Hartung, K. A. S. Al-Rasheid, S. Sonnewald, U. Sonnewald, S. Kneitz, N. Lachmann, R. R. Mendel, F. Bittner, A. M. Hetherington, R. Hedrich, The stomatal response to reduced relative humidity requires guard cell-autonomous ABA synthesis. *Curr. Biol.* **23**, 53–57 (2013).
25. K. Ohashi-Ito, D. C. Bergmann, *Arabidopsis* FAMA controls the final proliferation/differentiation switch during stomatal development. *Plant Cell* **18**, 2493–2505 (2006).
26. J. A. Anderson, S. S. Huprikar, L. V. Kochian, W. J. Lucas, R. F. Gaber, Functional expression of a probable *Arabidopsis thaliana* potassium channel in *Saccharomyces cerevisiae*. *Proc. Natl. Acad. Sci. U.S.A.* **89**, 3736–3740 (1992).
27. B. Muller-Rober, J. Ellenberg, N. Provart, L. Willmitzer, H. Busch, D. Becker, P. Dietrich, S. Hoth, R. Hedrich, Cloning and electrophysiological analysis of KST1, an inward rectifying K^+ channel expressed in potato guard cells. *EMBO J.* **14**, 2409–2416 (1995).
28. P. Ache, D. Becker, N. Ivashikina, P. Dietrich, M. R. G. Roelfsema, R. Hedrich, GORK, a delayed outward rectifier expressed in guard cells of *Arabidopsis thaliana*, is a K^+-selective, K^+-sensing ion channel. *FEBS Lett.* **486**, 93–98 (2000).
29. A. C. Wille, W. J. Lucas, Ultrastructural and histochemical-studies on guard cells. *Planta* **160**, 129–142 (1984).
30. M. R. G. Roelfsema, R. Steinmeyer, M. Staal, R. Hedrich, Single guard cell recordings in intact plants: light-induced hyperpolarization of the plasma membrane. *Plant J.* **26**, 1–13 (2001).
31. H. Marten, K. R. Konrad, P. Dietrich, M. R. G. Roelfsema, R. Hedrich, Ca^{2+}-dependent and -independent abscisic acid activation of plasma membrane anion channels in guard cells of *Nicotiana tabacum*. *Plant Physiol.* **143**, 28–37 (2007).
32. V. Levchenko, K. R. Konrad, P. Dietrich, M. R. G. Roelfsema, R. Hedrich, Cytosolic abscisic acid activates guard cell anion channels without preceding Ca^{2+} signals. *Proc. Natl. Acad. Sci. U.S.A.* **102**, 4203–4208 (2005).
33. A. Stange, R. Hedrich, M. R. G. Roelfsema, Ca^{2+}-dependent activation of guard cell anion channels, triggered by hyperpolarization, is promoted by prolonged depolarization. *Plant J.* **62**, 265–276 (2010).
34. Z. H. Chen, A. Hills, C. K. Lim, M. R. Blatt, Dynamic regulation of guard cell anion channels by cytosolic free Ca^{2+} concentration and protein phosphorylation. *Plant J.* **61**, 816–825 (2010).
35. S. G. Huang, R. Waadt, M. Nuhkat, H. Kollist, R. Hedrich, M. R. G. Roelfsema, Calcium signals in guard cells enhance the efficiency by which abscisic acid triggers stomatal closure. *New Phytol.* **224**, 177–187 (2019).
36. K. Raschke, H. Schnabl, Availability of chloride affects balance between potassium chloride and potassium malate in guard cells of *Vicia faba* L. *Plant Physiol.* **62**, 84–87 (1978).
37. F.-Q. Guo, J. Young, N. M. Crawford, The nitrate transporter AtNRT1.1 (CHL1) functions in stomatal opening and contributes to drought susceptibility in *Arabidopsis*. *Plant Cell* **15**, 107–117 (2003).
38. D. Geiger, S. Scherzer, P. Mumm, A. Stange, I. Marten, H. Bauer, P. Ache, S. Matschi, A. Liese, K. A. S. Al-Rasheid, T. Romeis, R. Hedrich, Activity of guard cell anion channel SLAC1 is controlled by drought-stress signaling kinase-phosphatase pair. *Proc. Natl. Acad. Sci. U.S.A.* **106**, 21425–21430 (2009).
39. R. Hedrich, I. Marten, Malate-induced feedback-regulation of plasma-membrane anion channels could provide a CO_2 sensor to guard cells. *EMBO J.* **12**, 897–901 (1993).
40. S. Meyer, P. Mumm, D. Imes, A. Endler, B. Weder, K. A. S. Al-Rasheid, D. Geiger, I. Marten, E. Martinoia, R. Hedrich, *At*ALMT12 represents an R-type anion channel required for stomatal movement in *Arabidopsis* guard cells. *Plant J.* **63**, 1054–1062 (2010).
41. S. Batool, V. V. Uslu, H. Rajab, N. Ahmad, R. Waadt, D. Geiger, M. Malagoli, C. B. Xiang, R. Hedrich, H. Rennenberg, C. Herschbach, R. Hell, M. Wirtz, Sulfate is incorporated into cysteine to trigger ABA production and stomatal closure. *Plant Cell* **30**, 2973–2987 (2018).
42. M. R. Blatt, Potassium-dependent, bipolar gating of K^+ channels in guard cells. *J. Membrane Biol.* **102**, 235–246 (1988).
43. M. R. G. Roelfsema, V. Levchenko, R. Hedrich, ABA depolarizes guard cells in intact plants, through a transient activation of R- and S-type anion channels. *Plant J.* **37**, 578–588 (2004).
44. Y. Wang, K. Noguchi, N. Ono, S. Inoue, I. Terashima, T. Kinoshita, Overexpression of plasma membrane H^+-ATPase in guard cells promotes light-induced stomatal opening and enhances plant growth. *Proc. Natl. Acad. Sci. U.S.A.* **111**, 533–538 (2014).
45. J. Falhof, J. T. Pedersen, A. T. Fuglsang, M. Palmgren, Plasma membrane H^+-ATPase regulation in the center of plant physiology. *Mol. Plant* **9**, 323–337 (2016).
46. M. R. Blatt, F. Armstrong, K^+ channels of stomatal guard-cells: Abscisic-acid-evoked control of the outward rectifier by cytoplasmic pH. *Planta* **191**, 330–341 (1993).
47. M. R. G. Roelfsema, H. B. A. Prins, The membrane potential of *Arabidopsis thaliana* guard cells; depolarizations induced by apoplastic acidification. *Planta* **205**, 100–112 (1998).
48. P. Maheshwari, S. M. Assmann, R. Albert, A guard cell abscisic acid (ABA) network model that captures the stomatal resting state. *Front. Physiol.* **11**, 927 (2020).
49. A. Hills, Z. H. Chen, A. Amtmann, M. R. Blatt, V. L. Lew, OnGuard, a computational platform for quantitative kinetic modeling of guard cell physiology. *Plant Physiol.* **159**, 1026–1042 (2012).
50. I. A. Newman, Ion transport in roots: Measurement of fluxes using ion-selective microelectrodes to characterize transporter function. *Plant Cell and Environ.* **24**, 1–14 (2001).
51. P. J. Franks, I. R. Cowan, G. D. Farquhar, A study of stomatal mechanics using the cell pressure probe. *Plant Cell and Environ.* **21**, 94–100 (1998).
52. H. M. Muller, N. Schafer, H. Bauer, D. Geiger, S. Lautner, J. Fromm, M. Riederer, A. Bueno, T. Nussbaumer, K. Mayer, S. A. Alquraishi, A. H. Alfarhan, E. Neher, K. A. S. Al-Rasheid, P. Ache, R. Hedrich, The desert plant *Phoenix dactylifera* closes stomata via nitrate-regulated SLAC1 anion channel. *New Phytol.* **216**, 150–162 (2017).
53. J. Brearley, M. A. Venis, M. R. Blatt, The effect of elevated CO_2 concentrations on K^+ and anion channels of *Vicia faba* L. guard cells. *Planta* **203**, 145–154 (1997).
54. Z. M. Pei, K. Kuchitsu, J. M. Ward, M. Schwarz, J. I. Schroeder, Differential abscisic acid regulation of guard cell slow anion channels in *Arabidopsis* wild-type and *abi1* and *abi2* mutants. *Plant Cell* **9**, 409–423 (1997).
55. M. R. G. Roelfsema, S. Hanstein, H. H. Felle, R. Hedrich, CO_2 provides an intermediate link in the red light response of guard cells. *Plant J.* **32**, 65–75 (2002).
56. A. Guzel Deger, S. Scherzer, M. Nuhkat, J. Kedzierska, H. Kollist, M. Brosche, S. Unyayar, M. Boudsocq, R. Hedrich, M. R. G. Roelfsema, Guard cell SLAC1-type anion channels mediate flagellin-induced stomatal closure. *New Phytol.* **208**, 162–173 (2015).

57. Y. Liu, T. Maierhofer, K. Rybak, J. Sklenar, A. Breakspear, M. G. Johnston, J. Fliegmann, S. G. Huang, M. R. G. Roelfsema, G. Felix, C. Faulkner, F. L. H. Menke, D. Geiger, R. Hedrich, S. Robatzek, Anion channel SLAH3 is a regulatory target of chitin receptor-associated kinase PBL27 in microbial stomatal closure. *eLife* **8**, 23 (2019).
58. M. R. Blatt, Potassium channel currents in intact stomatal guard-cells: rapid enhancement by abscisic acid. *Planta* **180**, 445–455 (1990).
59. Z. M. Pei, Y. Murata, G. Benning, S. Thomine, B. Klusener, G. J. Allen, E. Grill, J. I. Schroeder, Calcium channels activated by hydrogen peroxide mediate abscisic acid signalling in guard cells. *Nature* **406**, 731–734 (2000).
60. Y. Murata, Z. M. Pei, I. C. Mori, J. Schroeder, Abscisic acid activation of plasma membrane Ca^{2+} channels in guard cells requires cytosolic NAD(P)H and is differentially disrupted upstream and downstream of reactive oxygen species production in *abi1-1* and *abi2-1* protein phosphatase 2C mutants. *Plant Cell* **13**, 2513–2523 (2001).
61. K. Shimazaki, M. Iino, E. Zeiger, Blue light-dependent proton extrusion by guard-cell protoplasts of *Vicia faba*. *Nature* **319**, 324–326 (1986).
62. M. Hayashi, S. Inoue, K. Takahashi, T. Kinoshita, Immunohistochemical detection of blue light-induced phosphorylation of the plasma membrane H^+-ATPase in stomatal guard cells. *Plant Cell Physiol.* **52**, 1238–1248 (2011).
63. K. R. Konrad, T. Maierhofer, R. Hedrich, Spatio-temporal aspects of Ca^{2+} signalling: Lessons from guard cells and pollen tubes. *J. Exp. Bot.* **69**, 4195–4214 (2018).
64. K. K. Li, J. Prada, D. S. C. Damineli, A. Liese, T. Romeis, T. Dandekar, J. A. Feijó, R. Hedrich, K. R. Konrad, An optimized genetically encoded dual reporter for simultaneous ratio imaging of Ca^{2+} and H^+ reveals new insights into ion signaling in plants. *New Phytol.* **230**, 2292–2310 (2021).
65. N. Scholz, C. L. Guan, M. Nieberler, A. Grotemeyer, I. Maiellaro, S. Q. Gao, S. Beck, M. Pawlak, M. Sauer, E. Asan, S. Rothemund, J. Winkler, S. Promel, G. Nagel, T. Langenhan, R. J. Kittel, Mechano-dependent signaling by Latrophilin/CIRL quenches cAMP in proprioceptive neurons. *eLife* **6**, e28360 (2017).
66. Y. Zhou, M. Ding, X. Duan, K. R. Konrad, G. Nagel, S. Gao, Extending the anion Channelrhodopsin-based toolbox for plant optogenetics. *Membranes* **11**, 287 (2021).
67. K. A. Mott, T. N. Buckley, Patchy stomatal conductance: Emergent collective behaviour of stomata. *Trends Plant Sci.* **5**, 258–262 (2000).
68. K. A. Mott, D. Peak, Stomatal patchiness and task-performing networks. *Ann. Bot.* **99**, 219–226 (2007).
69. R. Hedrich, V. Salvador-Recatala, I. Dreyer, Electrical wiring and long-distance plant communication. *Trends Plant Sci.* **21**, 376–387 (2016).
70. E. E. Farmer, Y. Q. Gao, G. Lenzoni, J. L. Wolfender, Q. Wu, Wound- and mechanostimulated electrical signals control hormone responses. *New Phytol.* **227**, 1037–1050 (2020).
71. M. R. McAinsh, A. M. Hetherington, Encoding specificity in Ca^{2+} signalling systems. *Trends Plant Sci.* **3**, 32–36 (1998).
72. J. Dempster, A new version of the Strathclyde Electrophysiology software package running within the Microsoft Windows environment. *J. Physiol.-London* **504P**, P57 (1997).
73. J. Schindelin, I. Arganda-Carreras, E. Frise, V. Kaynig, M. Longair, T. Pietzsch, S. Preibisch, C. Rueden, S. Saalfeld, B. Schmid, J. Y. Tinevez, D. J. White, V. Hartenstein, K. Eliceiri, P. Tomancak, A. Cardona, Fiji: An open-source platform for biological-image analysis. *Nat. Methods* **9**, 676–682 (2012).
74. J. Bohm, S. Scherzer, E. Krol, I. Kreuzer, K. von Meyer, C. Lorey, T. D. Mueller, L. Shabala, I. Monte, R. Solano, K. A. S. Al-Rasheid, H. Rennenberg, S. Shabala, E. Neher, R. Hedrich, The Venus flytrap *Dionaea muscipula* counts prey-induced action potentials to induce sodium uptake. *Curr. Biol.* **26**, 286–295 (2016).
75. J. Dindas, S. Scherzer, M. R. G. Roelfsema, K. von Meyer, H. M. Muller, K. A. S. Al-Rasheid, K. Palme, P. Dietrich, D. Becker, M. J. Bennett, R. Hedrich, AUX1-mediated root hair auxin influx governs SCFTIR1/AFB-type Ca^{2+} signaling. *Nat. Commun.* **9**, 10 (2018).
76. T. Gutermuth, S. Herbell, R. Lassig, M. Brosche, T. Romeis, J. A. Feijo, R. Hedrich, K. R. Konrad, Tip-localized Ca^{2+}-permeable channels control pollen tube growth via kinase-dependent R- and S-type anion channel regulation. *New Phytol.* **218**, 1089–1105 (2018).

Acknowledgments

Funding: This work was supported by grants from the German Science Foundation (DFG) [KO3657/2-3 to K.R.K., RO2381/8-1 to M.R.G.R., and DFG Koselleck award to R.H. (HE1640/42-1)], King Saud University's International Cooperation and Scientific Twinning Department, Riyadh, Saudi Arabia (Project ICSTD-2020/2) to K.A.S.A.-R. and R.H., Prix-Louis-Jeantet 2013 to G.N., and the China Scholarship Council (CSC) to S.H. (201506350031) and M.D. (201706170081). **Author contributions:** K.R.K., G.N., S.G., R.H., M.R.G.R., M.D., K.A.S.A.-R., and S.H. designed the project. S.H., M.D., and S.S. performed the experiments. I.D. designed and conducted the mathematical modeling. M.D., S.H., S.S., and K.R.K. analyzed the data. S.H., M.D., I.D., K.A.S.A.-R., M.R.G.R., R.H., and K.R.K. wrote the manuscript. **Competing interests:** The authors declare that they have no competing interests. **Data and materials availability**: All data needed to evaluate the conclusions in the paper are present in the paper and/or the Supplementary Materials. Additional data related to this paper may be requested from the authors.

Submitted 8 January 2021
Accepted 26 May 2021
Published 9 July 2021
10.1126/sciadv.abg4619

Citation: S. Huang, M. Ding, M. R. G. Roelfsema, I. Dreyer, S. Scherzer, K. A. S. Al-Rasheid, S. Gao, G. Nagel, R. Hedrich, K. R. Konrad, Optogenetic control of the guard cell membrane potential and stomatal movement by the light-gated anion channel *Gt*ACR1. *Sci. Adv.* **7**, eabg4619 (2021).